

28 June 2009

## Raising Cavity Q for Microwave-Pulse Compression by Reducing Aperture Skin-Effect Losses

Carl E. Baum  
University of New Mexico  
Department of Electrical and Computer Engineering  
Albuquerque New Mexico 87131

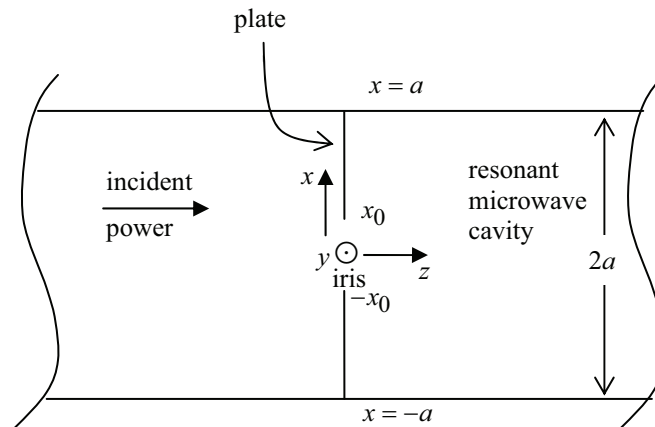
### Abstract

This paper discusses the losses in a waveguide-cavity oscillator. Particular attention is given to an inductive iris for feeding into (charging) the oscillator.

## 1. Introduction

In microwave pulse compression it is important to minimize losses in the resonant cavity. It is these losses which limit the power gain  $G$  in going from some source to the power in the resonant mode which will be switched into a load (e.g., antenna). Thinking of the resonant cavity as a length of shorted waveguide, the output pulse has a width of roughly the round trip transit time in the guide based on the group velocity, if the energy is switched out at one end. As discussed in [4] one can design a magic tee which can be used to take waveguide power in two directions and match it into a single output guide. This doubles the power out, but with the magic tee being in the center of the guide, the pulse width is halved.

Besides the losses in the waveguide walls there are losses at both ends and at any perturbations in the waveguide walls (probes, switch, magic tee, etc.). A common technique for feeding power into the waveguide cavity involves an iris as indicated in Fig. 1.1. The iris has width  $2x_0$  in the  $\pm x$  direction, and length  $2b$  (the full guide height in the  $\pm y$  direction). It is cut into what we can call the “plate”.



View perpendicular to broad wall

Fig. 1.1 Inductive Iris for Feeding Power into Waveguide Cavity.

## 2. Symmetry Decomposition of Magnetic Field

To simplify the analysis let us note that the incident power is much less than the power in the resonant cavity (Fig. 1.1). As illustrated in Fig. 2.1 we can then decompose the resonant cavity fields into symmetric and antisymmetric parts [5] with respect to the  $z = 0$  symmetry plane. Note that it is the magnetic fields here illustrated which are at right angles to the surface current density,  $\vec{J}_s$ , on the waveguide-discontinuity plane (in which the iris is placed).

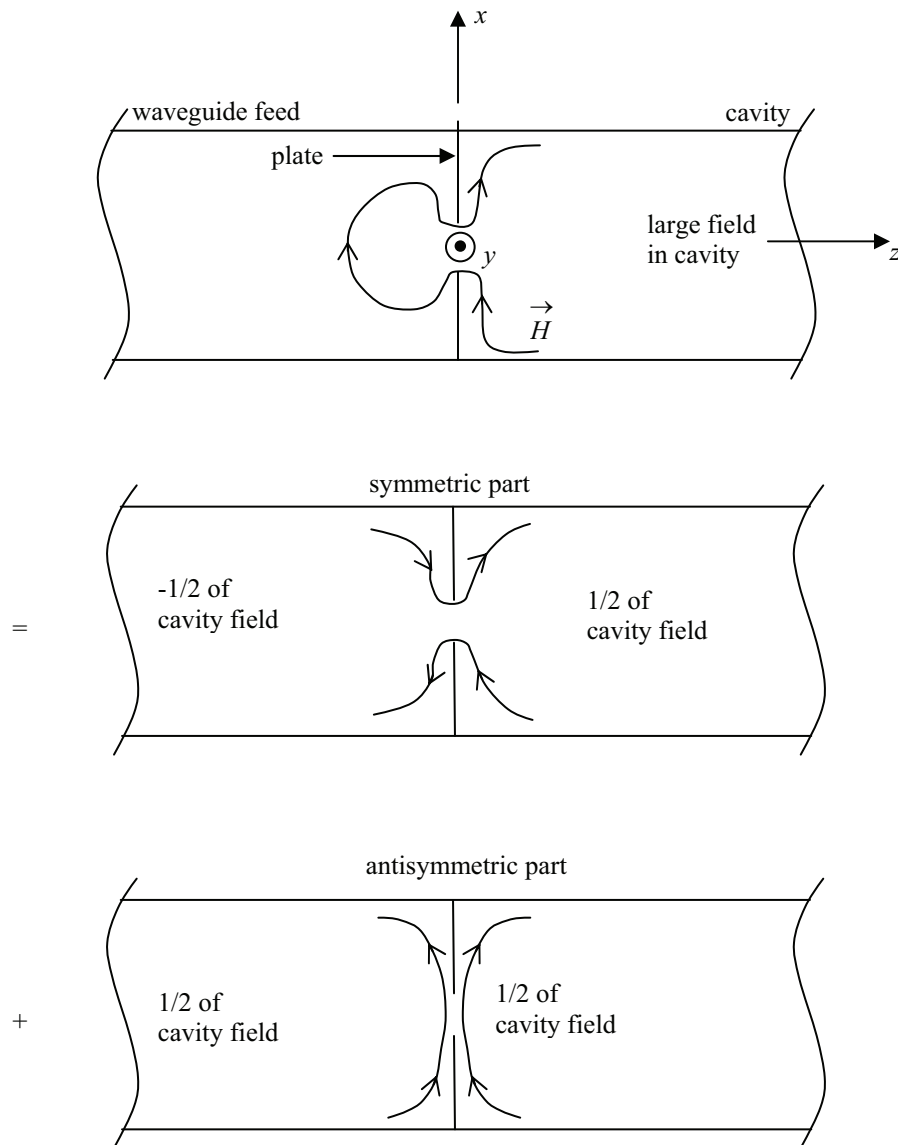


Fig. 2.1 Decomposition of Cavity Magnetic Field

### 3. Current Density and Power Loss Near Knife-Edge Boundary of Iris

This is discussed in [1-3]. In this case the surface current density near the edge behaves asymptotically as

$$\vec{J}_s = J_{s0} \left[ \frac{d}{x-x_0} \right]^{1/2} \vec{1}_y \quad \text{for } x > x_0 \quad (3.1)$$

using the coordinates in Fig. 1.1 for the edge at  $x = x_0$ . Here we have

$$\begin{aligned} J_{s0} (A/m) &= \text{order of } \vec{H} \text{ in cavity} \\ d (m) &= \text{scaling constant} \end{aligned} \quad (3.2)$$

There are of course, two such edges which will have the same effect due to symmetry. Our analysis will concentrate then on the half for  $x \geq 0$ .

To make a rough estimate of the additional power loss due to iris edges, let us first assume that

$$0 = \frac{x_0}{a} \ll 1 \quad (3.3)$$

so that we can approximate the surface current density on the shorted aperture as

$$\vec{J}_{s0} = J_{s0} \vec{1}_y \quad (3.4)$$

This is uniform (not a function of  $x$  or  $y$ ) and is on the  $+z$  side of the shorting plate. For the symmetric part (Fig. 2.1)

$$\vec{J}_s = J_s \vec{1}_y \rightarrow \frac{J_{s0}}{2} \vec{1}_y \quad \text{for } x \gg x_0 \quad (3.5)$$

in the same direction on both sides of the plate. For the antisymmetric part we have

$$\vec{J}_s = \pm J_{s0} \vec{1}_y \quad (+ \text{ for } z=0_+, - \text{ for } z=0_-) \quad (3.6)$$

with this applying all over the  $z = 0$  plane, except in the iris. The boundary conditions are exactly matched on both the plate (infinitesimally thick) and the aperture.

Figure 3.1 illustrates the symmetric part of the magnetic field near the aperture. For a conformal transformation we have

$$\begin{aligned}
 w(\zeta) &= u(\zeta) + jv(\zeta) \equiv \text{complex potential} \\
 u(\zeta) &\equiv \text{electric potential} \\
 v(\zeta) &\equiv \text{magnetic potential} \\
 \zeta &= x + jz \equiv \text{complex coordinate} \\
 v &= 0 \text{ on } x = 0 \text{ and on } z = 0 \text{ in aperture} \\
 u &= 0 \text{ on } z = 0 \text{ with } |x| > x_0
 \end{aligned}
 \tag{3.7}$$

The symmetries of this problem give us the simple results:

- a) The magnetic field at the origin is zero.
- b) For  $|x| < x_0$  on  $z = 0$  the magnetic field is perpendicular to the  $z = 0$  plane (and is an odd function of  $x$ ).
- c) For  $|x| > x_0$  on  $z = 0$  the magnetic field is parallel to the  $z = 0$  plane (oppositely directed on the two sides).
- d) The magnetic field is perpendicular to the  $x = 0$  plane for  $|x| < x_0$ .

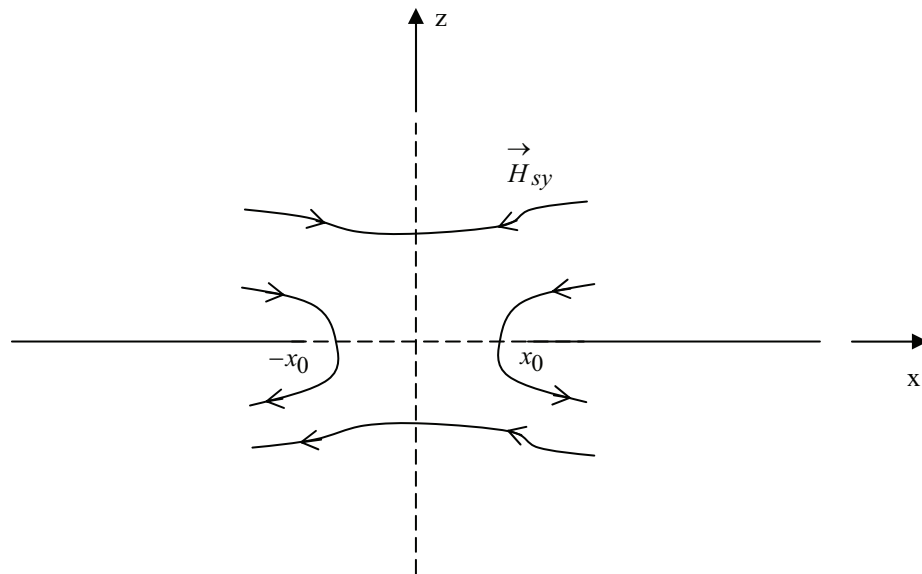


Fig. 3.1 Symmetric Part of Magnetic Field Near Aperture

Figure 3.2 gives a sequence of transformations. The aforementioned symmetries allow us to concentrate on the first quadrant of the  $\zeta$  plane ( $x \geq 0, y \geq 0$ ). In Fig. 3.2A the  $jz$  axis is rotated by  $\pi/2$  to the negative real ( $x_1$ ) axis. This is then shifted (Fig. 3.2B) to the left so that the conductor edge is moved to the origin. The negative  $x_2$  axis is then rotated (Fig. 3.2C) by  $-\pi/2$  to the  $jv$  axis. The magnetic field is now uniform and directed to the right. Summarizing, the final transformation gives

$$\begin{aligned} w &= \left[ \zeta^2 - x_0^2 \right]^{1/2}, \quad \zeta = \left[ w^2 + x_0^2 \right]^{1/2} \\ \frac{dw}{d\zeta} &= \zeta \left[ \zeta^2 - x_0^2 \right]^{-1/2}, \quad w^{-1} = \left[ w^2 + x_0^2 \right]^{-1/2} \end{aligned} \quad (3.8)$$

From (3.8) we have on the  $x$  axis

$$\begin{aligned} u &= \left[ x^2 - x_0^2 \right]^{1/2}, \quad v = 0 \quad \text{for } x \rightarrow x_0 \\ \frac{dw}{d\zeta} &= x \left[ x^2 - x_0^2 \right]^{-1/2} \rightarrow 1 \quad \text{as } x \rightarrow \infty \end{aligned} \quad (3.9)$$

From (3.5) the surface current density for the symmetric part goes to  $J_{s0}/2$  as  $x \rightarrow \infty$ . Hence we have the  $y$ -directed surface current density as

$$J_{s_y} = \frac{1}{2} J_{s0} \times \left[ x^2 - x_0^2 \right]^{-1/2}, \quad x > x_0 \quad (3.10)$$

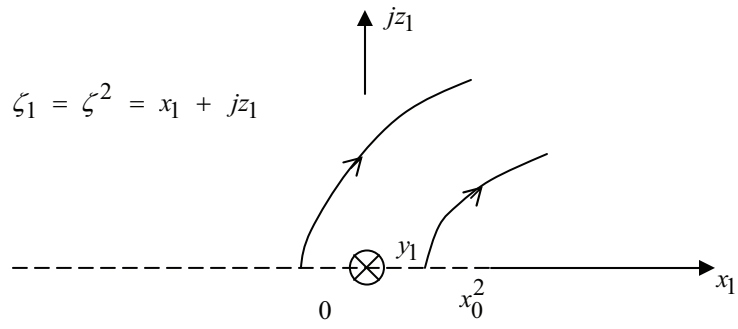
This applies equally to both sides of the  $z = 0$  plane.

Adding the antisymmetric part we have (for  $x > x_0$ )

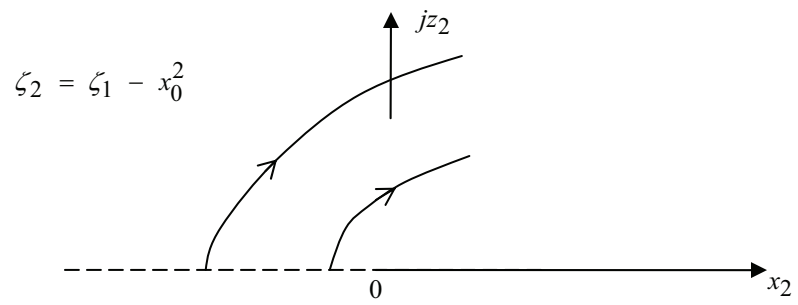
$$J_s = \begin{cases} \left[ \frac{1}{2} J_{s0} \left[ \left[ x^2 - x_0^2 \right]^{-1/2} + 1 \right] \right] & \text{for } z = 0_+ \\ \left[ \frac{1}{2} J_{s0} \left[ \left[ x^2 - x_0^2 \right]^{-1/2} - 1 \right] \right] & \text{for } z = 0_- \end{cases} \quad (3.11)$$

The power lost in the plate per unit width with no aperture is proportional to

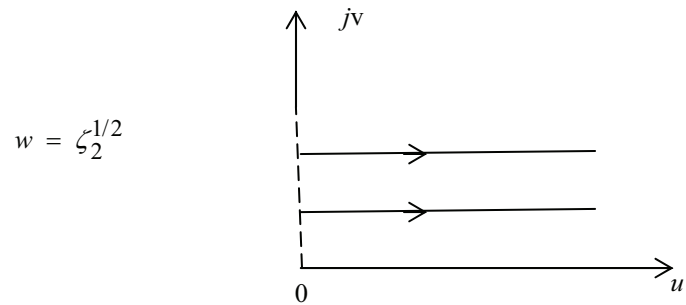
$$P_0 = J_{s0}^2 R_s x \quad (3.12)$$



A. First transformation (first quadrant to first two)



B. Second transformation (shift to left)



C. Third transformation (two quadrants to first)

Fig. 3.2 Conformal Transformation

taken out to some distance  $x$  (here considering the  $x > 0$  contribution). The power with the aperture is proportional to

$$P_1 = \int_{x_0}^x J_s^2 R_s dx \quad (3.13)$$

With this applying to both sides of the  $z = 0$  plane.

We then have

$$\begin{aligned} \Delta P &= \lim_{x \rightarrow \infty} P_1 - P_1 \\ &= \lim_{x \rightarrow \infty} J_{s_0}^2 R_s \left[ \int_{x_{0+}}^x \left[ \frac{1}{4} \left[ x \left[ x^2 - x_0^2 \right]^{-1/2} + 1 \right]^2 + \frac{1}{4} \left[ x \left[ x - x_0^2 \right]^{-1/2} - 1 \right]^2 \right] dx - x \right] \\ &= \lim_{x \rightarrow \infty} J_{s_0}^2 R_s \left[ \int_{x_{0+}}^x \left[ \frac{1}{2} \left[ x^2 \left[ x^2 - x_0^2 \right]^{-1} + 1 \right] dx - \int_{x_0}^x dx - x_0 \right] \right] \\ &= \lim_{x \rightarrow \infty} J_{s_0}^2 R_s \left[ \int_{x_{0+}}^x \frac{1}{2} \frac{x_0^2}{x^2 - x_0^2} dx - x_0 \right] \\ &= J_{s_0}^2 R_s \left[ \int_{x_{0+}}^x \frac{1}{2} \frac{x_0^2}{x^2 - x_0^2} dx - x_0 \right] \end{aligned} \quad (3.14)$$

where the integral is taken from  $x_{0+} > x_0$  because of the singularity. Changing variables we have

$$\begin{aligned} \xi &= \frac{x}{x_0}, \quad \frac{x_{0+}}{x_0} \equiv 1_+ \\ \int_{x_{0+}}^{\infty} \frac{x_0^2}{x^2 - x_0^2} dx &= x_0 \int_{1_+}^{\infty} \left[ \xi^2 - 1 \right]^{-1} d\xi \\ &= -x_0 \operatorname{arc coth}(\xi) \Big|_{1_+}^{\infty} \\ &= -\frac{x_0}{2} \ln \left( \frac{\xi + 1}{\xi - 1} \right) \Big|_{1_+}^{\infty} \\ &= \frac{x_0}{2} \ln \left( \frac{x_{0+} + x_0}{x_{0+} - x_0} \right) \end{aligned} \quad (3.15)$$



Defining

$$\Delta x = x_{0+} - x_0 \quad (3.16)$$

then we have

$$\Delta P = J_{s0}^2 R_s x_0 \left[ \frac{1}{4} \ell n \left( \frac{2x_0}{\Delta x} \right) - 1 \right] \quad \text{as } \Delta x \rightarrow 0 \quad (3.17)$$

So  $\Delta P \rightarrow \infty$  logarithmically, a weak singularity.

#### 4. Comparison to Power Loss in Plate with Closed Aperture

With the aperture closed ( $x_0 = 0$ ) the current on the plate is

$$\vec{J}_s = J_{s0} \cos \left( \frac{\pi x}{2a} \right) \quad (4.1)$$

for the  $H_{1,0}$ , mode. For the portion of the plate from  $x=0$  to  $a$  the power loss is

$$P_2 = \int_0^a J_{s0}^2 R_s \cos^2 \left( \frac{\pi x}{2a} \right) dx = J_{s0}^2 R_s \frac{a}{2} \quad (4.2)$$

For

$$0 < x_0 \ll a \quad (4.3)$$

then we have

$$\frac{\Delta P}{P_2} = \frac{2x_0}{a} \left[ \frac{1}{4} \ell n \left( \frac{2x_0}{\Delta x} \right) - 1 \right] \quad \text{as } \Delta x \rightarrow 0 \quad (4.4)$$

as the fractional increase in the power loss in the plate.

As a practical matter,  $\Delta x$  is not taken to zero due to the finite thickness of the plate. As an example let

$$\begin{aligned} \Delta x &= 1 \text{ mm (for 1 mm thick plate)} \\ 2a &= 16.5 \text{ cm (L band guide WR-650)} \\ x_0 &= \frac{a}{2} = 4.1 \text{ cm} \end{aligned} \tag{4.5}$$

This gives

$$\frac{\Delta P}{P_2} = \frac{2x_0}{a} \left[ \frac{1}{4} \ln(82) - 1 \right] \approx 0.1 \tag{4.6}$$

which is not a large effect.

There is some uncertainty in this result since there is some distribution of  $J_s$  around the aperture edge at  $x_0$ . There is less enhancement of  $J_s$  at the plate edge due to the finite thickness of the plate. For further reduction of this effect one can round the edges of the aperture and increase the plate thickness as in Fig. 4.1. The resulting plate thickness would be something on the order of  $x_0$  (more or less).

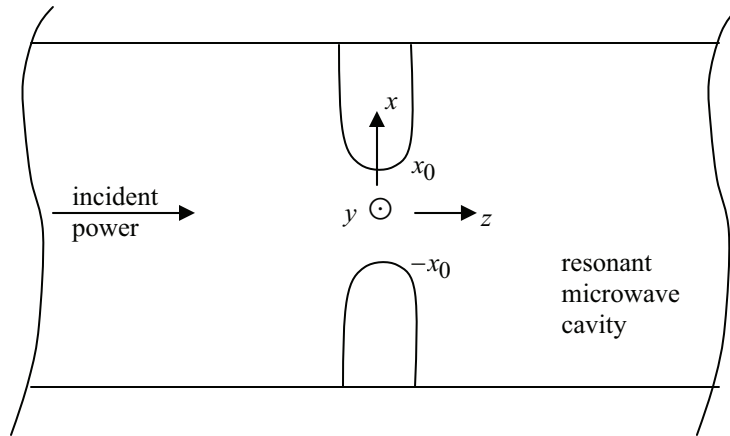


Fig. 4.1 Inductive Iris with Rounded Edges

## 5. Output-Port Skin-Effect-Loss Reduction

While the cavity is being rung up toward full field strength there are also losses in other discontinuities. One of these might be the H-plane bend output of a magic tee as in Fig. 5.1. As indicated, the junction can have rounded edges at the connection to the output waveguide. This applies not only to the narrow walls, but also to the broad walls. As discussed in [4] the height of the output guide might be less than that of the oscillator guide for impedance-matching purposes. In this case the broad-wall connection of the output guide to the oscillator guide can also be rounded.

Figure 5.1 also shows the connection of a possible input guide for charging the oscillator. The connection edges here can also be rounded.

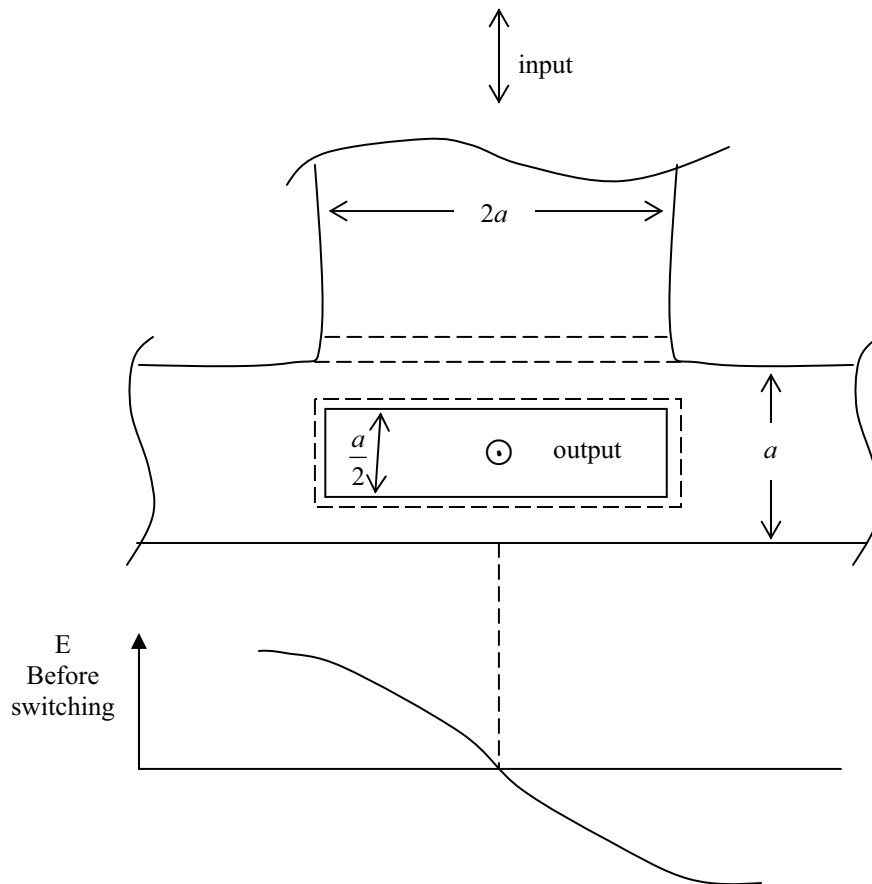


Fig. 5.1 Rounding Edges in magic Tee

## 6. Concluding Remarks

The general lesson is that sharp edges are to be avoided to minimize losses in the waveguide-cavity oscillator. This is not a large effect, but it helps.

## References

1. D. V. Giri and C. E. Baum, "Equivalent Displacement for a High-Voltage Rollup on the Edge of a Conducting Sheet", *Sensor and Simulation Note 294*, October 1986; INCEMIC 1987, Bangalore, India, September 1987, pp. 229-232.
2. C. E. Baum and J. S. Tyo, "Transient Skin Effect in Cables", *Measurement Note 47*, July 1996.
3. J. S. Tyo and C. E. Baum, "Reduced Skin Loss Dissipation at the Edges of a Conducting Plate Using High-Voltage Rollups", *Measurement Note 51*, April 1997.
4. C. E. Baum, "Impedance-Matched Magic Tee", *Circuit and Electromagnetic System Design Note 51*, March 2006.
5. C. E. Baum and H. N. Kritikos, "Symmetry in Electromagnetics", Ch. 1, pp. 1-90, in C. E. Baum and H. N. Kritikos (eds.), *Electromagnetic Symmetry*, Taylor & Francis, 1995.